Isolation of *Medicago truncatula* Mutants Defective in Calcium Oxalate Crystal Formation[1]

Paul A. Nakata* and Michele M. McConn

United States Department of Agriculture/Agricultural Research Service, Children's Nutrition Research Center, Department of Pediatrics, Baylor College of Medicine, 1100 Bates Street, Houston, Texas 77030–2600

Plants accumulate crystals of calcium oxalate in a variety of shapes, sizes, amounts, and spatial locations. How and why many plants form crystals of calcium oxalate remain largely unknown. To gain insight into the regulatory mechanisms of crystal formation and function, we have initiated a mutant screen to identify the genetic determinants. Leaves from a chemically mutagenized *Medicago truncatula* population were visually screened for alterations in calcium oxalate crystal formation. Seven different classes of calcium oxalate defective mutants were identified that exhibited alterations in crystal nucleation, morphology, distribution and/or amount. Genetic analysis suggested that crystal formation is a complex process involving more than seven loci. Phenotypic analysis of a mutant that lacks crystals, *cod 5*, did not reveal any difference in plant growth and development compared with controls. This finding brings into question the hypothesized roles of calcium oxalate formation in supporting tissue structure and in regulating excess tissue calcium.

Crystals of calcium oxalate are widespread among microorganisms, plants, and animals (Hodgkinson, 1977). They are formed from environmentally derived calcium and from biologically synthesized oxalate. In plants, calcium oxalate crystals are found in more than 215 families and often account for a substantial portion of the plant's dry weight (McNair, 1932). Oxalate-producing plants, which include many crop plants, accumulate oxalate in the range of 3%–80% (w/w) of their dry weight (Zindler-Frank, 1976; Libert and Franceschi, 1987).

Although crystal formation is common in plants, very little is known about the mechanisms regulating oxalate production and crystal formation (for review, see Webb, 1999). A number of pathways for oxalate production have been proposed. These pathways include the cleavage of isocitrate, hydrolysis of oxaloacetate, glycolate/glyoxylate oxidation, and/or oxidative cleavage of L-ascorbic acid (Hodgkinson, 1977). Of these pathways, the cleavage of ascorbic acid appears to be the most attractive (Yang and Loewus, 1975; Nuss and Loewus, 1978; Li and Franceschi, 1990; Keates et al., 2000). Once produced, the oxalate then combines with calcium to generate the vast variety of observed crystal shapes and sizes. The mechanism by which this process is controlled remains unknown. It has been suggested that a number of factors play a role in defining crystal shape and growth. These factors include macromolecules such as proteins, polysaccharides, and lipids as well as macromolecular membrane structures (Horner and Wagner, 1980; Arnott and Webb, 1983; Webb, 1999). Further studies are required to identify the pathway(s) of oxalate production and calcium oxalate crystal formation.

The diversity of crystal shapes and sizes, as well as their prevalence and spatial distribution, have led to a number of hypotheses regarding crystal function in plants. The proposed functions include roles in ion balance, in plant defense, in tissue support, in detoxification, and in light gathering and reflection (for review, see Franceschi and Horner, 1980). More extensive analysis is required to clarify the functional role(s) of calcium oxalate formation in plants.

Although crystal formation has intrigued scientists for many years, our knowledge about crystal formation is incomplete. Thus far, investigations into crystal formation and crystal function have relied primarily on biochemical (Franceschi et al., 1993; Webb et al., 1995) and cellular approaches (for review, see Arnott and Pautard, 1970; Franceschi and Horner, 1980; Zindler-Frank, 1987; Webb, 1999). Such studies have provided valuable information about the crystal ultrastructure and the developmental stages of crystal formation. These approaches, however, have been impeded by the relatively small number of crystal idioblasts (specialized calcium oxalate accumulating cells) present in a given tissue and by the technical difficulties associated with isolating intact crystal idioblasts in sufficient quantities for experimental study. A genetic approach would circumvent such technical limitations (e.g. idioblast number) and is a proven complement of biochemical and cellular investigations (Browse and Somerville, 1994; Schuma-

[1] This research was supported in part by the U.S. Department of Agriculture, Agricultural Research Service (under Cooperative Agreement no. 58–6250–6–001). The contents of this publication do not necessarily reflect the views or policies of the U.S. Department of Agriculture, nor does mention of trade names, commercial products, or organizations imply endorsement by the U.S. Government.

* Corresponding author; e-mail pnakata@bcm.tmc.edu; fax 713–798–7078.

cher and Chory, 2000). Mutant analysis would allow the identification of genes expressed at low levels or those only transiently expressed in the crystal idioblast. In addition, genetic analysis would provide insights into the functional role of each identified gene and into the sequential placement of each gene within the pathway(s) of crystal development.

In this study, we report the establishment of a genetic screen to investigate calcium oxalate formation in plants. In brief, leaves from a chemically mutagenized *Medicago truncatula* population were inspected for alterations in calcium oxalate deposition. Key attributes of *M. truncatula* include its short generation time, small genome size (3–4 times the size of Arabidopsis), ability to be transformed, autogamous and diploid nature, and spatial pattern of calcium oxalate crystal formation. *M. truncatula* is a model system for legumes, and thus many of the genetic and molecular tools that will be required for long-term genetic studies are under current development (Cook et al., 1997). Thus far our screen has led to the identification of a number of calcium oxalate defective (*cod*) mutants that display a variety of crystal phenotypes. These phenotypes include alterations in crystal nucleation, crystal morphology, crystal distribution, and/or crystal amount. Characterization of a mutant that lacks the ability to form crystals indicates that calcium oxalate formation is not required for normal growth and development under controlled greenhouse or growth chamber conditions. This observation challenges the hypotheses that crystal formation, at least in this species, is essential for calcium regulation and/or tissue support. The availability of *cod* mutants will allow the study of many aspects of crystal formation and function that have been previously inaccessible.

RESULTS

Genetic Model to Study Calcium Oxalate Formation

In selecting a plant genetic system suitable for investigating crystal formation, we had to identify a plant that could satisfy two criteria. First, the plant had to form crystals of calcium oxalate in an easily discernable pattern. Second, the plant had to be amenable to genetic study. Unfortunately, the simplest plant genetic model, Arabidopsis, adequately satisfied only the latter of the two requirements. Therefore, we inspected tissue harvested from a number of plants searching for a suitable model system. The model system we chose that satisfied both criteria was the forage crop *M. truncatula. M. truncatula* is currently being developed as a model legume system (Cook et al., 1997). Thus, many of the genetic tools required for long-term genetic study will be available.

Genetic Screen for *cod* Mutants

To establish the wild-type crystal accumulation pattern, tissue from various parts of the plant were visually inspected using the light microscope. Although crystals were observed in various parts of the plant, we decided to use leaves as the tissue source for our genetic screen. Upon inspections of wild-type leaves, prismatic crystals (twinned) were easily distinguished, accumulating along the vascular strands of secondary veins (Fig. 1, A and B). This defined pattern of vascular crystal accumulation would allow easier recognition of altered patterns of crystal formation. A comparison between young, expanding leaves and mature leaves revealed that the older leaves also accumulated small, globular-shaped crystals sparsely scattered throughout the mesophyll cells (Fig. 1, C and D).

To identify mutants in calcium oxalate crystal formation, M_2 populations of ethyl methanesulfonate (EMS)-mutagenized *M. truncatula* plants were screened for defects in crystal deposition. A single leaf from each of 6,653 M_2 plants was visually inspected for alterations in the pattern of crystal deposition. We predicted that this screening procedure would lead to the identification of *cod* mutants with alterations in crystal number, size, shape, and/or distribution pattern. Putative mutants identified by this screening procedure were transferred to soil and allowed to self-fertilize. The M_3 plants were then grown and the mutant phenotype confirmed. Although subtle differences exist (between plants of the same age), the *cod* mutants appeared generally similar to wild-type in overall growth and development (Fig. 2A). One noticeable exception was mutant *cod 4* (Fig. 2A), which appeared somewhat smaller and more chlorotic.

To determine the genetic basis of the individual mutants, each mutant was crossed with wild type. The resulting F_1 plants were analyzed for crystal phenotype, and all exhibited a wild-type crystal pattern indicating that each mutation was recessive. In addition, segregation analysis of the F_2 populations (Table I) fit the Mendelian expected ratio of 3:1 for a single recessive mutation. To determine if each mutant was a result of a mutation in a separate gene, complementation analysis was performed. The F_1 plants, generated from separate crosses between each mutant line, all exhibited a wild-type crystal phenotype. Thus, the seven *cod* mutants were determined to be non-allelic.

Change in Crystal Number and Distribution

Four mutants (*cod 3*, *cod 4*, *cod 5*, and *cod 6*) showed alterations in crystal number (Fig. 2B). Mutant *cod 5* lacked crystals, whereas *cod 6* accumulated fewer crystals than wild type. The *cod 6* mutant showed the same spatial calcium oxalate accumulation pattern as wild type by accumulating crystals along the vascular strand. The accumulated crystals, however, were

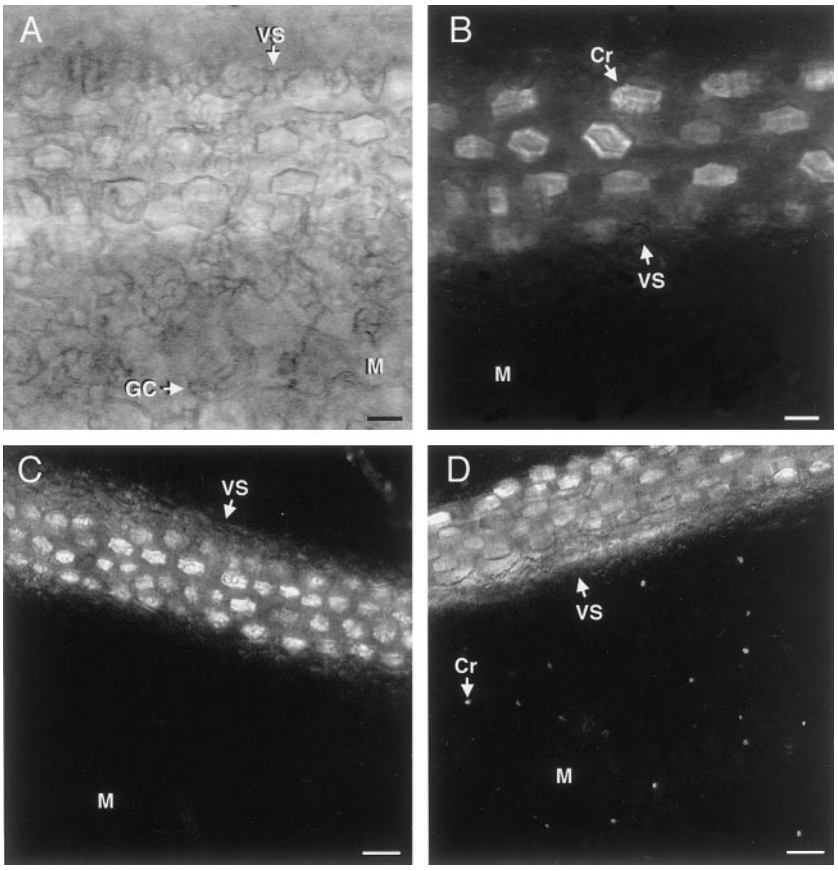

Figure 1. Crystal development in leaves of *M. truncatula*. Leaves were harvested, cleared, and visually inspected using light microscopy. A representative region of a secondary vein and surrounding mesophyll is shown in A, B, C, and D. A single expanding leaf (cleared whole mount) is shown under bright field (A) and between crossed polarizers (B). Scale bar = 10 μm. Prismatic calcium oxalate crystal (white coffin-shaped structures) were observed accumulating exclusively along the vascular strand. A whole-mount comparison between an expanding leaf (C) and a fully expanded leaf (D) is shown between crossed polarizers. In addition to the prismatic crystals present along the vascular strand, small globular-shaped crystals (white spots) were observed sparsely distributed within the mesophyll cells of the more mature leaf (D). Scale bar = 20 μm. VS, Vascular strand; GC, guard cell; M, mesophyll; Cr, calcium oxalate crystal.

smaller, globular in shape, and fewer in number. The *cod 5* mutant did not accumulate crystals along the vascular strand.

The increase in crystal number observed in *cod 3* and *cod 4* was attributed to an increase in the spatial distribution of calcium oxalate accumulation. Like wild-type plants, *cod 3* and *cod 4* accumulated crystals along the vascular strand; however, they also accumulated crystals within mesophyll cells (Fig. 2B). Although wild-type plants are capable of crystal formation within the mesophyll cells, crystals are not observed until much later in development. Mutant *cod 4* exhibited normal prismatic crystal development along the vascular strand and globular-shaped crystals within many of its mesophyll cells. To eliminate the possibility that the globular-shaped structures were simply starch aggregates, leaves from *cod 4* were separately incubated in Lugol solution and in ethanol/commercial bleach (Ilarslan et al., 1997). Each incubation indicated that the globular structures were not starch (data not shown). On the other hand, mutant *cod 3* exhibited thin wafer-like crystals within both the vascular strand and more globular-shaped crystals within the mesophyll cells.

Change in Crystal Shape and Size

Several mutants (*cod 1*, *cod 2*, *cod 3*, *cod 6*, and *cod 7*) exhibited a change in crystal shape and size (Fig. 2B). Large diamond-shaped crystals were observed in *cod 1*. Mutant *cod 3* also showed diamond-shaped crystals along the vascular strand and globular-shaped crystals within the mesophyll cells. These crystals, however, were much smaller and thinner. Kinked rectangular crystals were observed in *cod 2*. In addition to having an altered shape, the *cod 2* crystals also appeared much thinner than the wild-type prismatic crystals. Mutant *cod 6* not only had fewer crystals, but also exhibited crystals that were much smaller and appeared as spots along the vascular strand. The crystal profile of *cod 7* resembled wild type in general shape, but showed unusual globular protrusions from the crystal surface, which we speculate may represent additional nucleation sites.

Oxalate and Calcium Content

Measurements were conducted to determine if oxalate levels correlated with the observed changes in crystal accumulation (Table II). Measurements of wild-type leaves showed a total oxalate level of about 21 mg g^{-1} dry weight with the majority of the tissue oxalate residing in the insoluble form (calcium oxalate). The insoluble oxalate was determined to be the calcium salt by energy dispersive x-ray elemental analysis conducted on isolated crystals (data not shown). Although altered in crystal morphology, the

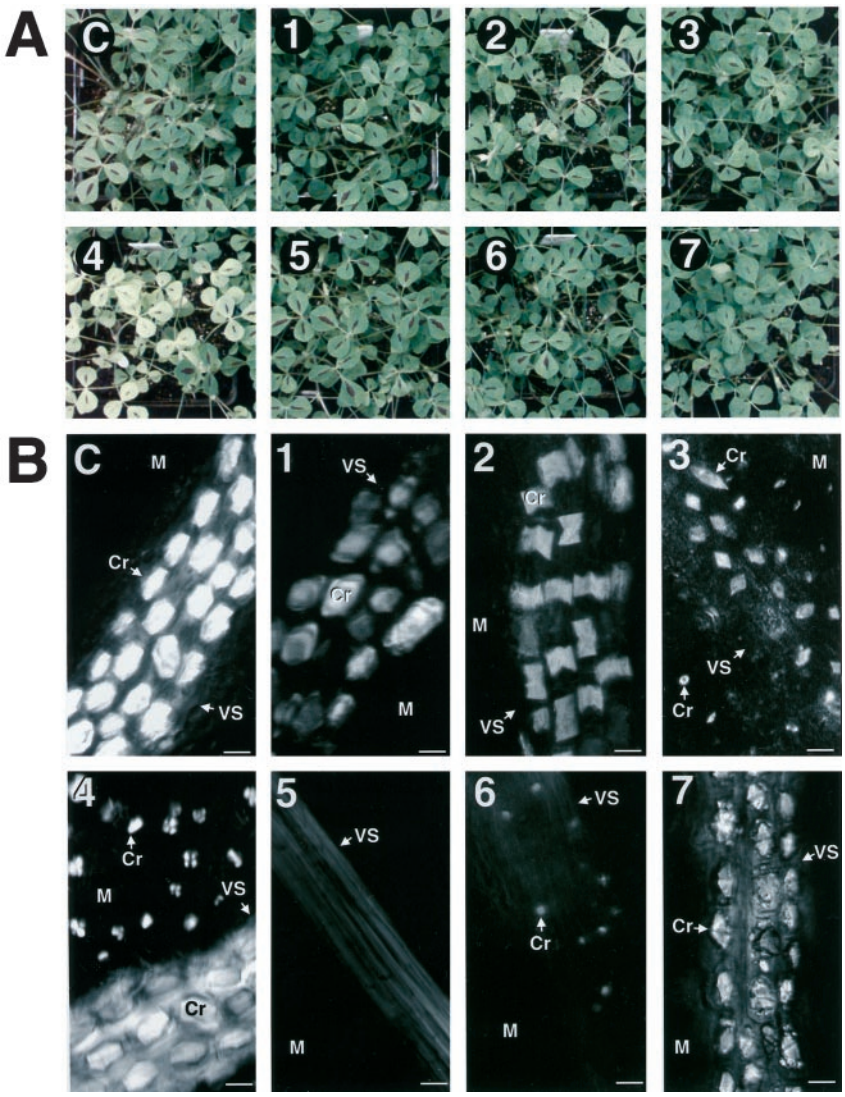

Figure 2. *cod* mutants. A, Control plant (C) and individual *cod* mutants (1–7) grown under greenhouse conditions. B, A representative portion of a whole-mount leaf clearing, showing a secondary vein and surrounding mesophyll cells, from the control plant and each *cod* mutant (1–7) are shown under polarizing optics. Crystals appear as bright spots. The mutants *cod 1*, *cod 4*, and *cod 5* showed changes in crystal number compared with controls. Mutants *cod 3*, *cod 4*, and *cod 5* showed changes in the pattern of crystal distribution. Changes in crystal size were observed in *cod 1*, *cod 3*, and *cod 6*, whereas changes in crystal shape were observed in *cod 1*, *cod 2*, *cod 3*, *cod 6*, and *cod 7*. All mutants shown were backcrossed a minimum of two times and are of the same age. VS, Vascular strand; M, mesophyll; Cr, calcium oxalate crystal. Scale bars = 10 μm.

two mutants, *cod 1 and cod 7*, showed a crystal pattern and size similar to those of wild type and likewise had levels of oxalate similar to that of wild type. The two mutants, *cod 5* and *cod 6*, which showed a decrease in crystals, also exhibited a corresponding reduction in the total amount of oxalate. Oxalate levels were barely detectable in *cod 6* and at the level of detection in *cod 5*. Measurements conducted on *cod 2* also showed a reduction in oxalate level. Thus, the reduction in oxalate levels may be attributed to a decrease in thickness and size of the individual crystals (Fig. 2). Mutant *cod3* and *cod 4* showed an increase in the total amount of oxalate.

Measurements were conducted to assess whether calcium levels corresponded with changes in the amount of oxalate (Table III). Levels did vary, but no

Table I. *Segregation analysis of the cod mutants*

Mutant	F_1 (Mutant × WT[a]) Phenotype	F_2 Segregation (WT:Mutant)	Expected Ratio (WT:Mutant)	χ^2	*P*
cod 1	WT	117:34	3:1	0.50	0.48
cod 2	WT	111:33	3:1	0.33	0.56
cod 3	WT	218:69	3:1	0.14	0.70
cod 4	WT	444:159	3:1	0.60	0.44
cod 5	WT	115:39	3:1	0.01	0.93
cod 6	WT	151:48	3:1	0.08	0.77
cod 7	WT	108:40	3:1	0.32	0.57

[a] WT, Wild type.

mutant showed any substantial reduction in the amount of calcium compared with control plants (approximately 20 mg g^{-1} dry weight). This finding, along with the widely varying calcium oxalate levels, indicated that some of the isolated mutants have drastically altered the amount of calcium they sequester as the oxalate salt.

DISCUSSION

Genetic analysis of the *cod* mutants (*cod 1*, *cod 2*, *cod 3*, *cod 6*, and *cod 7*) revealed that a single point mutation can result in a variety of different crystal shapes and sizes. Although the specific genes that have been altered are not yet known, the results show that the control of crystal morphology is complex (five different loci identified thus far) and under strict genetic control. As suggested by studies in other systems, mutations affecting protein, lipid, or polysaccharide function could all contribute to alterations in crystal size or shape. We currently are generating plants that contain multiple mutations. Analysis of the resulting plants will provide further insight into the genetic mechanisms regulating crystal nucleation, growth, and morphology.

A variety of functional roles have been hypothesized for calcium oxalate formation, based on the natural variation in crystal number, morphology, and distribution that exists among different plant species. Roles in ion balance (e.g. calcium regulation), in tissue support, in plant defense, in light gathering and reflection, and in detoxification have all been proposed (Franceschi and Horner, 1980). Calcium regulation (for review, see Franceschi and Loewus, 1995) and plant defense (Thurston, 1976), however, are the only proposed roles supported by experimental data. Studies in support of a role in calcium regulation have shown that calcium oxalate crystals rapidly increase in size and number as the concentration of calcium in the plant environment is increased (Zindler-Frank, 1975; Franceschi and Horner, 1979; Borchert, 1985, 1986; Franceschi, 1989). The possibility that this high-calcium sequestration system evolved to prevent intracellular calcium toxicity through the formation of the osmotically and physiologically inert calcium oxalate crystal is intriguing. When grown in soil under greenhouse conditions, *M. truncatula* sequesters about 34% (w/w) of its total leaf calcium as crystals of calcium oxalate (calculated using measured values from Tables II and III). The sequestration of such a large percentage of calcium in the crystalline form suggests that the amount of calcium is in excess of what is needed for leaf growth and cellular function. Like control plants, leaves from the *cod 5* mutant had comparable calcium levels. In contrast to control plants, the *cod 5* mutant does not sequester calcium in the crystalline form. This lack of crystals did not appear to cause any change in growth or physical characteristics of the *cod 5* plant. This finding indicates that, under the growth conditions used in this study, calcium oxalate formation is not essential for normal growth and development in *M. truncatula*. Alternatively, it is possible that the *cod 5* mutation confers another mechanism(s) of calcium regulation that compensates for the lack of crystals. Further analysis of the mutants under a variety of different environmental conditions/regimes (e.g. calcium, other minerals, light, temperature, water stress, etc.) is required before a definitive conclusion can be drawn.

Another hypothesis that is not supported by observations of *cod 5* is a role for calcium oxalate formation in supporting tissue structure. The lack of an observable difference in leaf or plant rigidity between *cod 5* and wild-type plants suggests that calcium oxalate formation does not play a crucial role in the support of tissue structure, at least in *M. truncatula*. Overall, the different *cod* mutants isolated in this study will allow the systematic examination of these and other hypothesized roles for calcium oxalate formation.

Table II. *Oxalate content in leaves*

Leaves from control and each *cod* mutant were harvested from 8-week-old plants, frozen in liquid nitrogen, and freeze dried. Oxalate measurements were conducted on weighed leaf samples using an enzymatic assay. Values represent averages from three independent experiments each conducted in duplicate (mean ± SE).

Mutant	Calcium Oxalate	
	Insoluble	Soluble
	mg g^{-1} dry wt	
Control	21.4 ± 0.8	1.4 ± 0.2
cod 1	23.6 ± 0.9	1.3 ± 0.2
cod 2	8.6 ± 0.5	1.2 ± 0.4
cod 3	29.6 ± 0.7	1.4 ± 0.1
cod 4	35.1 ± 4.3	1.4 ± 0.3
cod 5	0.3 ± 0.3	1.0 ± 0.2
cod 6	1.9 ± 0.4	0.6 ± 0.1
cod 7	20.3 ± 0.4	1.5 ± 0.2

Table III. *Calcium content in leaves*

Leaves from control and each *cod* mutant were harvested from 8-week-old plants, frozen in liquid nitrogen, and freeze dried. Calcium measurements were conducted on weighed leaf samples using atomic absorption spectrophotometry. Values represent averages from three independent experiments each conducted in duplicate (mean ± SE). Data are from mutants reselected after at least two back crosses; *cod 4* and *cod 5* were backcrossed four times and three times, respectively.

Mutant	Calcium
	mg g^{-1} dry wt
Control	19.9 ± 0.7
cod 1	18.0 ± 0.1
cod 2	18.9 ± 0.5
cod 3	20.9 ± 0.2
cod 4	19.2 ± 1.1
cod 5	16.9 ± 0.2
cod 6	17.6 ± 0.9
cod 7	18.0 ± 0.4

In addition to providing insight into calcium oxalate formation and function in plants, the developed genetic system will also benefit studies investigating the effects of oxalates on human health. Nutritional studies have shown that oxalate is an anti-nutrient that sequesters calcium in a state that renders it unavailable for nutritional absorption by humans (Weaver et al., 1987; Heaney and Weaver, 1989; Weaver et al., 1997). The impact of oxalates on calcium bioavailability is important, considering the reliance of different populations around the world on plant foods as their main source of calcium and the failure of many in the United States to meet the recommended daily allowance for calcium intake (Lau et al., 1991; Weaver et al., 1997). Moreover, it has been suggested that the contribution of dietary oxalate to urinary oxalate excretion is more substantial than previously thought (Holmes and Assimos, 1998). Calcium oxalate crystals are the primary component of most urinary stones (Baggio and Gambaro, 1995). Thus besides increasing the nutritional quality, the ability to reduce the amount of oxalate in plant foods would also decrease a potentially toxic compound. The mutants that vary in the amount of oxalate suggest that the genetic manipulation of oxalate levels in plants is feasible. In addition, such forage crop mutants will allow the direct testing of biomedical and nutritional issues associated with crystal formation via animal feeding studies.

MATERIALS AND METHODS

Plant Materials

Medicago truncatula cv Jemalong ecotype A17 was used in this study. All seeds were generously provided by Dr. Douglas Cook (Texas A&M University, College Station). Seeds were removed from their pods, acid scarified (concentrated H_2SO_4), rinsed in water, and sown in the appropriate medium. Plants were then grown under greenhouse conditions.

Genetic Screen

EMS-mutagenized M_2 *M. truncatula* seeds were generously provided by Dr. Douglas Cook. Details on the mutagenesis procedure have been presented by Penmetsa and Cook (2000). Individual plants were grown in Cone-tainers (Hummert International, Earth City, MO) packed with vermiculite. The cone-tainers were then racked into sets of 200, watered with a nutrient solution [1.2 mM KNO_3, 0.8 mM $Ca(NO_3)_2$, 0.3 mM KH_2PO_4, 0.2 mM $MgSO_4$, 25 μM $CaCl_2$, 25 μM H_3BO_3, 2 μM $MnSO_4$, 2 μM $ZnSO_4$, 0.5 μM $CuSO_4$, 0.5 μM H_2MoO_4, 0.1 μM $NiSO_4$, 0.04 μM $CoCl_2$, and 50 μM Fe(III)-citrate], and grown under greenhouse conditions. After 3 to 4 weeks, leaf samples from each plant were harvested, cleared in acetone, and visually inspected for alterations in calcium oxalate crystal deposition (compared with wild type) using light microscopy. Images of whole leaf mounts were captured using a CCD72 camera mounted on a light microscope (Axiophot, Zeiss, Jena, Germany).

Segregation and Complementation Analysis

Segregation analysis was performed as described by Koornneef and Stam (1991). In brief, each isolated mutant was crossed with wild type (*M. truncatula* cv Jemalong ecotype A17). The F_1 seeds were planted and allowed to self-fertilize. The resulting F_2 seeds were then planted and scored for the crystal phenotype. The χ^2 and P values were obtained by using the statistical program CHITEST from Excel (Microsoft, Redmond, WA). Complementation analysis was conducted by reciprocal crosses between the individual mutants. The resulting F_1 seeds were then planted and scored for the crystal phenotype.

Mutant Backcrosses

Each isolated M_2 mutant was backcrossed to A17 to aid in the removal of secondary mutations. All reported analyses were conducted using plants that were backcrossed a minimum of two times. We have since verified all crystal phenotypes and oxalate measurements with plants backcrossed a minimum of four times.

Oxalate Measurements

Oxalate levels were determined by a method similar to that of Ilarslan et al. (1997). Tissue samples from 8-week-old plants, grown in soil under greenhouse conditions, were harvested and freeze-dried. Dried samples were then weighed, ground in water, and centrifuged. The supernatant was decanted and analyzed for soluble oxalate levels using an oxalate diagnostic kit (catalog no. 591–D, Sigma, St. Louis). Total oxalate levels were determined by simply omitting the centrifugation step and solubilizing the crystals. Crystals were solubilized by the addition of H^+-Dowex (catalog no. 50 × 8–400, Sigma) in dilute acid. The mixture was heated at 60°C for 1 h to dissolve the oxalate crystals. The pH of the mixture was then adjusted (pH 5–7), followed by charcoal filtration and centrifugation. The supernatant was then analyzed for oxalate content according to the manufacturer's instructions (Sigma). In brief, the oxalate was oxidized by oxalate oxidase to carbon dioxide and hydrogen peroxide. The generated hydrogen peroxide was then allowed to react with 3-methyl-2-benzothiazolinone hydrazone and 3-(dimethylamino) benzoic acid in the presence of peroxidase to give an indamine dye that was read at 590 nm. The values determined via the enzymatic oxalate kit were verified by HPLC according to Keates et al. (2000). Standards were prepared from oxalic acid dihydrate (Sigma) and used for both soluble and total oxalate measurements as recommended by the manufacturer. All plants used in these experiments were backcrossed at least twice. Measurements were done in duplicate on three independently grown sets of plants (seven mutant lines and one control), the results averaged, and SE calculated. Each set contained five plants for each mutant and control.

Calcium Measurements

Plants were grown in soil for 8 weeks under greenhouse conditions. Leaves were harvested, freeze-dried, and stored dessicated. Weighed tissue samples were wet digested with a nitric/perchloric acid mixture by heating to 150°C to 200°C while under vacuum until dry (Grusak, 1994). The dry digests were dissolved in 1 M nitric acid, incubated for 1 h, and diluted with distilled water. To determine the amount of calcium, each sample was analyzed by atomic absorption spectrophotometry (model 2100, Perkin Elmer, Norwalk, CT). All plants used in these experiments were backcrossed at least twice. Each measurement was done in duplicate on three independently grown sets of plants, the results averaged, and SE calculated. Each set contained five plants for each mutant and control.

ACKNOWLEDGMENTS

We are indebted to Dr. Douglas Cook for providing the EMS-mutagenized bulks of *M. truncatula* seeds. We are also grateful to Dr. Douglas Cook and Dr. R. Varma Penmetsa for their helpful discussions on the propagation of *M. truncatula*. We would like to thank Drs. John Browse, Vince Franceschi, and Thomas Okita for critical reading of the manuscript.

Received May 23, 2000; accepted August 9, 2000.

LITERATURE CITED

Arnott HJ, Pautard FGE (1970) Calcification in plants. *In* H Schraer, ed, Biological Calcification: Cellular and Molecular Aspects. Appleton-Century-Crofts, New York, pp 375–446

Arnott HJ, Webb MA (1983) Twin crystals of calcium oxalate in the seed coat of the kidney bean. Protoplasma **114:** 23–34

Baggio B, Gambaro G (1995) Cellular abnormalities of oxalate transport in nephrolithiasis. *In* SR Khan, ed, Calcium Oxalate in Biological Systems. CRC Press, Boca Raton, FL, p 207

Borchert R (1985) Calcium-induced patterns of calcium-oxalate crystals in isolated leaflets of *Gleditsia triacanthos* L. and *Albizia julibrissin* Durazz. Planta **165:** 301–310

Borchert R (1986) Calcium acetate induces calcium uptake and formation of calcium-oxalate crystals in isolated leaflets of *Gleditsia tracanthos* L. Planta **168:** 571–578

Browse J, Somerville CR (1994) Glycerolipids. *In* EM Meyerowitz, CR Somerville, eds, Arabidopsis. Cold Spring Harbor Laboratory Press, New York, pp 881–912

Cook CR, VandenBosch K, deBruijn FJ, Huguet T (1997) Model legumes get the nod. Plant Cell **9:** 275–281

Franceschi VR (1989) Calcium oxalate formation is a rapid and reversible process in *Lemna minor* L. Protoplasma **148:** 130–137

Franceschi VR, Horner HT Jr (1979) Use of *Psychotria puncata* callus in study of calcium oxalate crystal idioblast formation. Z Pflanzenphysiol **67:** 61–75

Franceschi VR, Horner HT Jr (1980) Calcium oxalate crystals in plants. Bot Rev **46:** 361–427

Franceschi VR, Li X, Zhang D, Okita TW (1993) Calsequestrin-like calcium binding protein is expressed in calcium accumulating cells of *Pistia stratiotes* L. Proc Natl Acad Sci USA **90:** 6986–6990

Franceschi VR, Loewus FA (1995) Oxalate biosynthesis and function in plants and fungi. *In* SR Khan, ed, Calcium Oxalate in Biological Systems. CRC Press, Boca Raton, FL, pp 113–130

Grusak MA (1994) Iron transport to developing ovules of *Pisum sativum*: I. Seed import characteristics and phloem iron-loading capacity of source regions. Plant Physiol **104:** 649–655

Heaney RP, Weaver CM (1989) Oxalate: effect on calcium absorbability. Am J Clin Nutr **50:** 830–832

Hodgkinson A (1977) Oxalic acid metabolism in higher plants. *In* A Hodgkinson, ed, Oxalic Acid Biology and Medicine. Academic Press, New York, pp 131–158

Holmes RP, Assimos DG (1998) Glyoxylate synthesis and its modulation and influence on oxalate synthesis. J Urol **160:** 1617–1624

Horner HT, Wagner BL (1980) The association of druse crystals with the developing stomium of *Capsicum annuum* (Solanaceae) anthers. Am J Bot **67:** 1347–1360

Ilarslan H, Palmer RG, Imsande J, Horner HT (1997) Quantitative determination of calcium oxalate in developing seeds of soybean (Leguminosae). Am J Bot **84:** 1042–1046

Keates SA, Tarlyn N, Loewus FA, Franceschi VR (2000) L-Ascorbic acid and L-galactose are sources of oxalic acid and calcium oxalate in *Pistia stratiotes*. Phytochemistry **53:** 433–440

Koornneef M, Stam P (1991) Genetic analysis. *In* C Koncz, NH Chua, J Schell, eds, Methods in Arabidopsis Research. World Scientific, River Edge, NJ, pp 83–99

Lau EMC, Cooper C, Woo J (1991) Calcium deficiency: a major cause of osteoporosis in Hong Kong Chinese. *In* P Burkhardt and RP Heaney, eds, Nutritional Aspects of Osteoporosis. Serono Symposium Publications from Raven Press, New York **85:** 175–180

Li XX, Franceschi VR (1990) Distribution of peroxisomes and glycolate metabolism in relation to calcium oxalate formation in *Lemna minor* L. Eur J Cell Biol **51:** 9–16

Libert B, Franceschi VR (1987) Oxalate in crop plants. J Agric Food Chem **35:** 926–938

McNair JB (1932) The interrelations between substances in plants: essential oils and resins, cyanogen and oxalate. Am J Bot **19:** 255–271

Nuss RF, Loewus FA (1978) Further studies on oxalic acid biosynthesis in oxalate-accumulating plants. Plant Physiol **61:** 590–592

Penmetsa RV, Cook DR (2000) Production and characterization of diverse developmental mutants of *Medicago truncatula*. Plant Physiol **123:** 1387–1397

Schumacher K, Chory J (2000) Brassinosteroid signal transduction: still casting the actors. Curr Opin Plant Biol **3:** 79–84

Thurston EL (1976) Morphology, fine structure and ontogeny of the stinging emergence of *Tragia ramosa* and *T. saxicola* (Euphorbiaceae). Am J Bot **63:** 710–718

Weaver CM, Heaney RP, Nickel KP, Packard PI (1997) Calcium bioavailability from high oxalate vegetables: Chinese vegetables, sweet potatoes and rhubarb. J Food Sci **62:** 524–525

Weaver CM, Martin BR, Ebner JS, Krueger CA (1987) Oxalic acid decreases calcium absorption in rats. J Nutr **117:** 1903–1906

Webb MA (1999) Cell-mediated crystallization of calcium oxalate in plants. Plant Cell **11:** 751–761

Webb MA, Cavaletto JM, Carpita NC, Lopez LE, Arnott HJ (1995) The intravacuolar organic matrix associated with calcium oxalate crystals in leaves of *Vitis*. Plant J **7:** 633–648

Yang J, Loewus FA (1975) Metabolic conversion of L-ascorbic acid in oxalate-accumulating plants. Plant Physiol **56:** 283–285

Zindler-Frank E (1975) On the formation of the pattern of crystal idioblasts in *Canavalia ensiformis* D.C.: VII. Calcium and oxalate content of the leaves in dependence of calcium nutrition. Z Pflanzenphysiol **77:** 80–85

Zindler-Frank E (1976) Oxalate biosynthesis in relation to photosynthetic pathways and plant productivity: a survey. Z Pflanzenphysiol **80:** 1–13

Zindler-Frank E (1987) Calcium oxalate in legumes. *In* E Stirton, ed, Advances in Legume Systematics, Part 3. Royal Botanic Gardens, Kew, UK, pp 279–316